(20) See the discussion of section 9.11.4.1 in: Birks, J. B., Ed. "Organic Molecular Photophysics"; Wiley: London, 1975; Vol. 2. In the context of molecular crystals there are two parameters that are considered: (1) τ_h, the hopping rate, and (2) c, the number of new sites visited by the exciton on each hop (in the limit of many hops). Thus while τ_h is found to be of the order of 0.1–0.3 ns, c is in the range 19–38, which is much larger than would be the case for a polymer. Hence there is some doubt as to whether the comparison of crystal and polymer τ_h values is meaningful.

Addition of Difluorocarbene to 1,4-Polybutadienes. Synthesis and Characterization of Novel Copolymers

S. Siddiqui and R. E. Cais*

AT&T Bell Laboratories, Murray Hill, New Jersey 07974. *Received September 23, 1985*

ABSTRACT: Difluorocarbene, generated under mild neutral conditions, adds cleanly to 1,4-*cis*- and -*trans*-polybutadienes to give cyclopropanated materials with complete retention of the double bond configuration. The addition can be effected to any desired degree of conversion by controlling the molar ratio of carbene precursor to the double bond, thus providing a series of novel copolymers. These fluorine-containing materials were characterized by thermal analysis, gel permeation chromatography, and high-field ^1H, ^{13}C, and ^{19}F NMR spectroscopy. The olefinic carbon resonances give the most detailed fine structure, which has been fully assigned to monomer sequence pentads. The addition of difluorocarbene takes place randomly to give a perfectly Bernoullian monomer sequence distribution, as well as an atactic stereosequence distribution.

Introduction

A carbene derives its important synthetic applications from cyclopropanation in a single key step in many target natural products, often with remarkable control of stereochemistry. A variety of carbenes have been shown to undergo reactions with double bonds along polymer backbones in much the same way as in simple alkenes.

Prior studies of the addition of methylene as well as dichlorocarbene to polybutadienes have been reported in the literature.[1,2] However, analogous reactions with difluorocarbene have not been examined heretofore. Surface modification of some polymer matrices by difluorocarbene has been claimed, despite lack of evidence of any direct chemical attachment of carbene fragments to the polymer.[3]

In the present study we examine the scope of the addition reaction of difluorocarbene ($:CF_2$) to both 1,4-*cis*- and -*trans*-polybutadienes. Since $:CF_2$ has a singlet ground-state electronic structure, it is possible to obtain these adducts without loss of the original configuration; i.e., the cis precursor polymer is expected to give only a cis adduct and the trans polymer a trans adduct. The properties of these novel fluoro copolymers depend on composition, which can be varied according to the extent of addition. High resolution multinuclear NMR methods are utilized to characterize the detailed microstructures of these materials.

Experimental Section

Materials. 1,4-*cis*-Polybutadiene (*cis*-PBD) was obtained from Aldrich Chemical Co. 1,4-*trans*-Polybutadiene (*trans*-PBD) was synthesized according to a literature procedure.[4] Both polymers had at least 98% isomeric purity as determined by ^{13}C NMR. (Trifluoromethyl)phenylmercury ($PhHgCF_3$) was obtained in about 40% overall yield from phenylmercuric hydroxide by the procedure of Seyferth.[5] Sodium iodide (Gold Label, 99.999% purity) was purchased from Aldrich and dried for 24 h at 140 °C under vacuum prior to use. Benzene and toluene were dried according to standard techniques and stored over molecular sieves under a nitrogen atmosphere. *cis*- and *trans*-5-decenes were obtained with better than 97% isomeric purity from Wiley Organics and used without further purification.

General Procedure for Cyclopropanation. The desired isomer of 1,4-polybutadiene was dissolved in either benzene or toluene (1% w/v)) with constant stirring under nitrogen. (Trifluoromethyl)phenylmercury (0.35–3.0 equiv with respect to double bonds) and dry sodium iodide (threefold molar excess with respect to $PhHgCF_3$) were added simultaneously to the polymer solution at room temperature. The mixture was vigorously stirred and heated to 80 °C, after which the reaction could be followed by the disappearance of $PhHgCF_3$ by TLC. Typical reaction times ranged from 20 to 30 h.

At the end of the reaction, the mixture was cooled to room temperature and filtered to remove insoluble materials (e.g., NaI, NaF, PhHgI, etc.). The filtrate was concentrated to one-third its original volume, whereupon more crystals of PhHgI appeared and were separated by centrifugation. The polymer was precipitated in a large excess of methanol containing 2,6-di-*tert*-butyl-4-methylphenol as an antioxidant, collected, washed several times with methanol, and dried overnight under vacuum. The polymer was then purified by dissolving in chloroform and reprecipitating in methanol. The conversion of double bonds was determined from 500-MHz ^1H spectra (vide infra). If further double bond conversion was desired, the partially cyclopropanated material could be recycled through the above operation without any degradation.

Samples of *cis*- and *trans*-1,2-di-*n*-butyl-3,3-difluorocyclopropane were obtained by the above procedure from the respective olefins. Distillation under reduced pressure (20 torr) gave analytical samples of these compounds.

Analytical Methods. Molecular weights ($\bar{M}_w$ and $\bar{M}_n$) were measured by gel permeation chromatography on a Waters liquid chromatograph fitted with μ-Styragel columns and calibrated with monodisperse polystyrene standards. Thermal gravimetric analyses (TGA) were performed on a Du Pont 1090 thermal analyzer with a DSC cell and a Du Pont 951 thermal gravimetric analysis attachment.

NMR Measurements. The 500-MHz proton (^1H) NMR spectra of all samples were acquired at room temperature on a JEOL GX-500 spectrometer. Typically, a 7–10% (w/v) polymer solution in $CDCl_3$ was used. The extent of cyclopropanation was calculated by integration of the appropriate proton resonances.

The 50.31-MHz carbon-13 NMR spectra were recorded at 50 °C on a Varian XL-200 spectrometer, from $CDCl_3$ solutions containing at least 15% (w/v) polymer. The internal reference was tetramethylsilane (Me_4Si), and about 10 000 transients were accumulated with a sweep width of 10 kHz in 32K of memory. Pulse repetition times were 5–15 s between 90° pulses (19.5-μs duration), and broad band proton decoupling was used. All quantitations were done with the integrated intensities of protonated carbons only.

The ^{13}C spin–lattice relaxation times (T_1) and nuclear Overhauser enhancements (NOE) were determined in order to choose appropriate delay times ($>5T_1$) for quantitatiion, and to deduce

0024-9297/86/2219-0595$01.50/0

dynamic information about the polymer. T_1 measurements employed the standard 180°–τ–90° inversion–recovery sequence,[6] with a recovery delay between 90° pulses greater than $5T_1$. Seven τ values were used for each T_1 determination. NOE measurements were carried out by using the gated decoupling technique. The DEPT (distortionless enhancement by polarization transfer) experiment was performed on partially cyclopropanated materials in order to assign carbon types (e.g., methylene, methine, etc.). The pulse sequence described by Doddrell et al.[7] was used.

Fluorine-19 NMR data were collected at 188.22 and 470.5 MHz with Varian XL-200 and JEOL GX-500 spectrometers, respectively. Typically, 200 transients were acquired from 7–10% (w/v) polymer solutions in $CDCl_3$ in a 5-mm sample tube at room temperature, using hexafluorobenzene (HFB) as an internal chemical shift reference ($\Phi^* = -163$ ppm). Sweep widths of 20 kHz and 50 kHz were used, with 32K and 64K computer data points for the 188.22- and 470.5-MHz spectra, respectively. A 7.5-s delay between 90° pulses was used in both cases, and ^1H–^{19}F scalar coupling was removed by broad-band decoupling.

Results and Discussion

Generation of Difluorocarbene. Of all the difluorocarbene precursors,[8] (trifluoromethyl)phenylmercury, developed by Seyferth,[5] appeared the most attractive since this reagent is readily prepared by a two-step procedure (see eq 1) and it can be stored for some time at ambient

$$\text{PhHgOH} + 48\%\ \text{HF} \rightarrow \text{PhHgF·HF}$$
$$\text{PhHgF·HF} + \text{PhHgCBr}_3 \rightarrow \text{PhHgCF}_3 \qquad (1)$$

temperature. The reagent releases difluorocarbene in the presence of sodium iodide as a nucleophile in a nonpolar solvent at ca. 80 °C. If the generation of $:CF_2$ is carried out in the presence of a trap like an olefin, the reaction provides an efficient way of synthesizing *gem*-difluorocyclopropanes.

Thus, when either *cis*- or *trans*-PBD is used as a $:CF_2$ trap, novel cyclopropanated materials can be obtained (see eq 2). This methodology utilizes rather mild, neutral

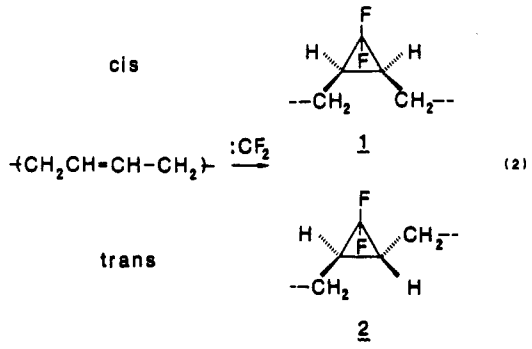

conditions, unlike the traditional generation of some dihalocarbenes under strongly basic conditions.[9] This nonbasic synthetic approach is preferred since it has been noted recently by Dias and others[10] that polybutadiene undergoes facile isomerization in the presence of a strong base. Nevertheless, dichlorocarbene generated in a highly basic medium reportedly adds to polybutadienes in a stereospecific manner, with no evidence of double bond isomerization prior to $:CCl_2$ addition.[1]

The present procedure for gem difluorocyclopropanation of polybutadienes is heterogeneous in nature but takes place efficiently with vigorous stirring. Moreover the consumption of $PhHgCF_3$ can be qualitatively followed by TLC. The extent of cyclopropanation is controlled by adjusting the molar ratio of $PhHgCF_3$ to unsaturation in the polymer backbone. Thus, a series of copolymers having different monomer compositions can be realized by this method.

As expected of a singlet carbene,[11] $:CF_2$ addition to polybutadienes proceeds without change of the double bond geometry; i.e., *cis*-PBD results in copolymers (henceforth termed as *cis*-PBD:CF_2 adducts) where the cyclopropyl substituents retain the cis configuration. Likewise, the adduct of *trans*-PBD (*trans*-PBD:CF_2) did not contain any cis cyclopropanated segments. The absence of mixtures of geometrical isomers in each case was proven by NMR analyses. However, the copolymers are not stereoregular (vide infra).

Table I
Glass Transitions, Crystalline Melting Temperatures, and Molecular Weights of Difluorocarbene Adducts of 1,4-Polybutadienes

% conversion of sample	T_g, °C	T_m, °C	$\bar{M}_w$	$\bar{M}_n$
		cis-PBD:CF_2		
0	−99.5	−9.3	5.24×10^5	1.08×10^5
18.1	−89.7			
27.6	−68.4			
68.4	−37.9			
97.4	−3.2	52.5	7.94×10^5	2.23×10^5
		trans-PBD:CF_2		
0	−85.0	119.0	1.45×10^5	1.28×10^4
20.7	−59.1	35.6		
62.6	−32.7			
87.0	−14.3	55.6		
98.0	−7.5	82.5	7.76×10^4	2.45×10^4

The addition of difluorocarbene to the polybutadienes occurs without any degradation of chain length, as shown by the molecular weight determinations (Table I). Futhermore, $:CF_2$ addition improves the stability of PBD. Examination by TGA shows that after complete reaction of the double bonds *cis*-PBD:CF_2 and *trans*-PBD:CF_2 are stable up to 300 and 350 °C, respectively. Above these temperatures weight loss takes place, presumably due to the evolution of HF. As the extent of propanation progresses in the polymer backbone, T_g increases linearly with composition as expected for a random copolymer.[12] Crystallinity, as manifested by T_m, is destroyed for intermediate compositions that have highly irregular chains that cannot pack well into a lattice. The results of T_g and T_m values for different copolymers are summarized in Table I.

The ^{13}C relaxation parameters (T_1 and NOE) were determined to monitor the effect of reaction on chain dynamics, as well as to establish proper conditions for quantitative measurements (see Table II). The chain motions are highly anisotropic as evidenced by the deviation of the methine/methylene T_1 ratio from 2.[13] Furthermore, the steady drop in T_1 values for each carbon with increasing reaction results from longer segmental correlation times owing to decreased chain mobility. This finding is in accord with the increasing T_g values noted above. The NOE values are near maximum for all protonated carbons, showing that chain motions are fast enough to be on the short correlation time side of the T_1 minimum.[14]

Proton NMR of *cis*- and *trans*-PBD:CF_2 Adducts. The 500-MHz proton NMR spectra of *cis*- as well as *trans*-PBD:CF_2 adducts at any degree of conversion do not exhibit sequence fine structure. Rather fortuitously, resonances from cyclopropyl methine protons (>CH–) and methylene protons (–CH_2–) on carbons next to the ring in *cis*-PBD:CF_2 copolymers overlap to give a broad singlet centered at 1.43 ppm (Figure 1, spectrum a). However, these resonances are clearly separated for *trans*-PBD:CF_2 adducts where the cyclopropyl methine protons appear upfield ($\delta_{>CH}$ 1.12) from methylene protons adjacent to the ring (δ_{-CH_2} 1.58) (Figure 1, spectrum b). In both cases,

Table II
T_1 (s) and NOE Relaxation Parameters of PBD:CF_2 from ^{13}C NMR

% conversion of sample	CH=		>CF_2		CH_2CH=		>CH		CH_2<	
	T_1	NOE	T_1	NOE	T_1	NOE	T_1	NOE	T_1	NOE
					cis-PBD:CF_2					
0	2.95	2.76			2.19	2.88				
27.6	2.62	2.85	2.66	1.09	1.86	2.88	1.68	2.97	1.19	2.93
68.4	1.40	2.85	2.19	1.06	1.04	2.90	1.15	2.85	0.74	2.92
97.4			1.62	1.05			0.83	2.84	0.56	2.90
					trans-PBD:CF_2					
0	2.44	2.66			1.10	2.80				
20.7	2.35	2.70	2.58	1.06	1.06	2.85	1.43	2.84	0.91	2.89
62.6	1.77	2.73	2.12	1.01	0.78	2.86	1.13	2.77	0.76	2.84
98.0			1.60	1.00			0.80	2.77	0.50	2.88

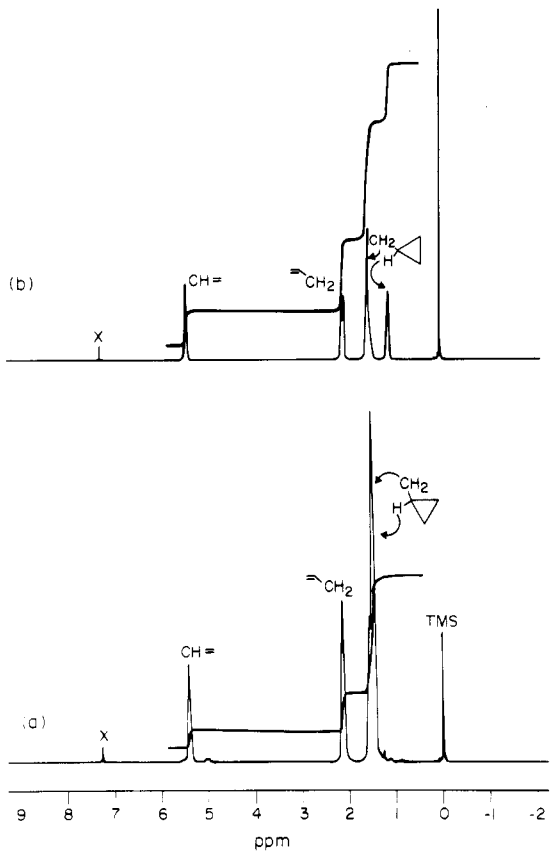

Figure 1. 500-MHz ^1H NMR of (a) *cis*-PBD:CF_2, and (b) *trans*-PBD:CF_2 adducts, observed in $CDCl_3$ at room temperature. x = $CHCl_3$.

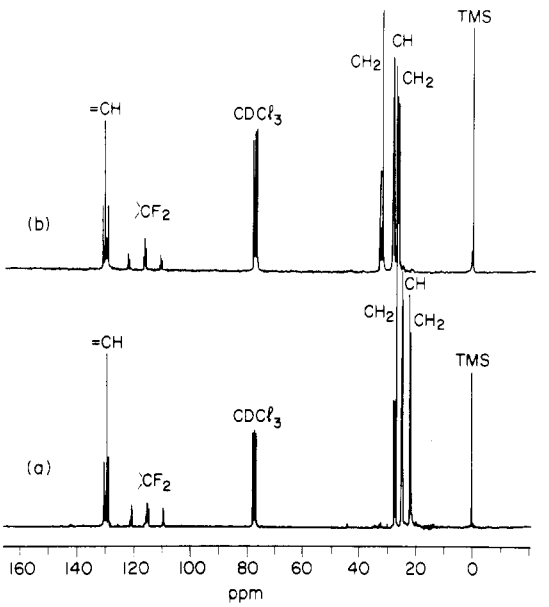

Figure 2. 50.3-MHz ^{13}C NMR spectra of (a) *cis*-PBD:CF_2, and (b) *trans*-PBD:CF_2 adducts observed in $CDCl_3$ at 50 °C.

allylic and olefinic protons from unreacted double bonds are well separated from the rest of the proton resonances. Thus, despite the lack of microstructural detail, ^1H NMR provided the simplest method for measuring the degree of conversion by integration of appropriate peak areas (see Figure 1). These ^1H NMR analyses compared very well with subsequent determinations by ^{13}C NMR spectra.

General Features of Carbon-13 NMR Spectra of *cis*- and *trans*-PBD:CF_2 Adducts. The 50.31-MHz ^{13}C NMR spectra of both *cis*-PBD:CF_2 and *trans*-PBD:CF_2 exhibit three distinct chemical shift regions corresponding to aliphatic, *gem*-difluoromethylene and olefinic carbon resonances (see Figure 2). The protonated carbons were assigned by spectral editing with the DEPT experiment.[7] The difluoromethylene carbon resonance is a multiplet owing to scalar ^{13}C–^{19}F coupling, with the following $^1J(^{13}C$–$^{19}F)$ values: *cis*-PBD:CF_2, 283 Hz; *trans*-PBD:CF_2, 288 Hz. The geometry of the cyclopropyl ring is revealed by the fluorine coupling pattern imposed on these ^{13}C resonances. Since the fluorines in *cis*-PBD:CF_2 adducts are nonequivalent (see structure 1, eq 2), the difluoromethylene carbon exhibits an AXY splitting pattern and appears as two sets of doublets with slightly different ^1J values. However, these fluorines are equivalent in *trans*-PBD:CF_2 at low degrees of conversion (see structure 2, eq 2), so that the difluoromethylene carbon resonance is a simple triplet ($^1J(^{13}C$–$^{19}F)$ = 288 Hz).

The above assignments were substantiated by observing the ^{13}C spectra of *cis*- and *trans*-1,2-di-*n*-butyl-3,3-difluorocyclopropanes (compounds **3** and **4**, respectively),

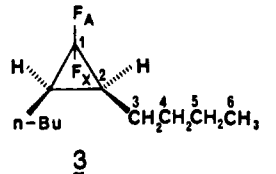

3

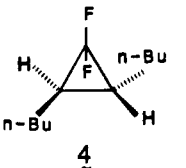

4

which were synthesized as model compounds for the copolymers under investigation. The 50.3-MHz ^{13}C spectrum of compound **3** observed in $CDCl_3$ at 50 °C exhibits the following carbon resonances relative to Me_4Si (for carbon numbering, see structure **3**): δ 13.96 (C-1, s), 31.70 (C-5, s), 22.46 (C-4, s), 21.40 (C-3, t, $^3J(^{13}C$–$^{19}F)$ = 3 Hz), 25.19 (C-2, t, $^2J(^{13}C$–$^{19}F)$ = 10.3 Hz), 118.64 (C-1, d, $^1J(^{13}C$–$^{19}F)$ = 284.5 Hz), 112.84 (C-1, d, $^1J(^{13}C$–$^{19}F)$ = 283.8 Hz). The *gem*-difluoromethylene carbon gives an AXY pair of doublets for the reasons stated above, with $^1J(^{13}C$–$^{19}F)$ values of 284.5 and 283.8 Hz, respectively. The cyclopropyl methine carbon shows a triplet splitting ($^2J(^{13}C$–$^{19}F)$ = 10.3

Table III
^{13}C Chemical Shifts of Aliphatic Carbons of *cis*-PBD:CF_2 Adducts (See Figure 3)[a]

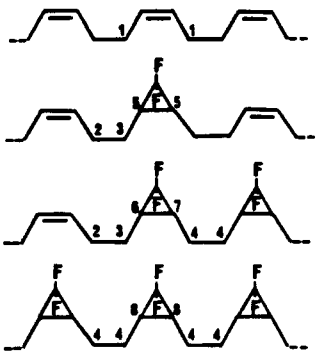

peak assignt	sequence	chem shift vs. Me_4Si, ppm
1	DD	27.51[b]
		27.45
2	DC, CD	26.94
3	DC, CD	21.87
4	CC	21.51
	(*m* and *r*)	21.33
5	DCD	24.92
	(mainly triplet)	24.72
		24.52
6	DCC (*m* and *r*)	24.91
7	CCD (*m'* and *r'*)	24.87
		24.71
		24.50
8	CCC	24.84
	(*rr'*, *rm'*, *mm'*, and *mr'*)	24.63
		24.46
		24.27

[a] Structural formulas for sequence determinations are shown. [b] The fine splittings may arise from the presence of either higher order monomer sequence or long-range ^{13}C–^{19}F coupling.

Hz) and the methylene carbon next to the ring experiences a small three-bond coupling ($^3J(^{13}C–^{19}F)$ ca. 3 Hz). The remaining carbon assignments for **3** are based upon chemical shift prediction rules.[15,16]

The ^{13}C NMR spectrum of the trans model compound **4** is essentially the same as that for **3**, except for the $–CF_2–$ carbon resonance, which is a simple triplet centered at 116.93 ppm ($^1J(^{13}C–^{19}F)$ = 288 Hz) as expected, and the methylene carbon next to the ring, which has no resolved splitting expected from three-bond fluorine coupling.

It is significant that the ^{13}C resonances for the cyclopropyl methine and the methylene carbons next to the ring for *cis*-PBD:CF_2 adducts always appear upfield from the resonances of their counterparts in *trans*-PBD:CF_2 adducts (see Figure 2 and Table III). These resonances are very useful for identifying the isomeric form of the cyclopropyl rings, which almost completely (>98%) retain the double bond configuration upon carbene addition.

Detailed Carbon-13 Microstructure of *cis*-PBD:CF_2 Adducts. The ^{13}C spectra of three *cis*-PBD:CF_2 adducts having 27.6%, 68.4%, and 97.6% conversions illustrate the microstructural features of interest. The assignments and structural formulas are given in Tables III–V, corresponding to Figures 3–5, respectively. The notation D and C represents unreacted ($–CH_2CH{=}CHCH_2–$) and reacted ($–CH_2\overline{CH}–\overline{CH}CH_2$) units, respectively. Figure 4 shows ^{13}C fine structure that arises from two kinds of methylene carbons as well as from cyclic methine carbons. Careful examination of the spectra reveals monomer sequence senstivity at the diad level for both methylene carbons; cyclopropyl ring carbons clearly exhibit monomer sequence triads. The chemical shifts corresponding to all possible sequences are assigned and compiled in Table III.

Table IV
^{13}C Chemical Shifts of Difluoromethylene (>CF_2) Carbon of *cis*-PBD:CF_2 (See Figure 4)[a]

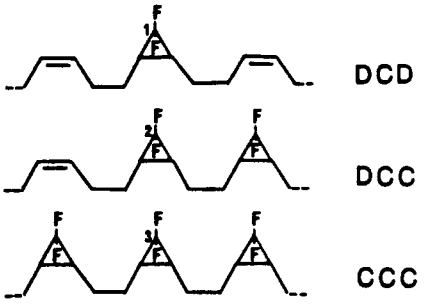

peak design.	assignt	chem shifts vs. Me_4Si, ppm
1	DCD	121.10
	(AXY quartet)	115.48
		115.29
		109.63
2	DCC	120.86
	(AXY quartet)	115.22
		115.05
		109.41
3	CCC	120.55
	(AXY quartet)	114.92
		114.74
		109.11

[a] Structural formulas for sequence determinations are shown.

Table V
^{13}C Chemical Shifts of Olefinic Carbons of *cis*-PBD:CF_2 Copolymers (See Figure 5)[a]

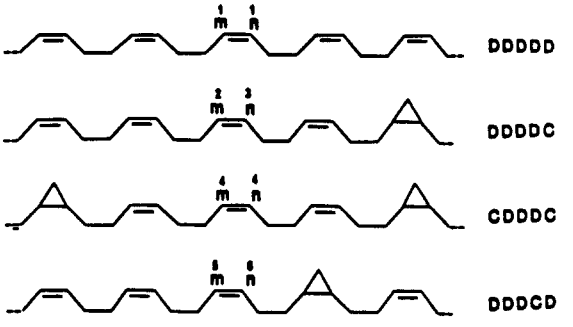

peak assignt	C-type sequence	chem shift vs. Me_4Si, ppm
1	DDDDD-*m,n*	129.68
2	DDDDC-*m*	129.79
3	DDDDC-*n*	129.54
4	CDDDC-*m,n*	129.54
5	DDDCD-*m*	130.41
6	DDDCD-*n*	128.81
7	CDDCD-*m*	130.27
8	CDDCD-*n*	128.92
9	DDDCC-*m*	130.53
10	DDDCC-*n*	128.69
11	CDDCC-*m*	130.38
12	CDDCC-*n*	128.84
13	DCDCD-*m,n*	129.55
14	DCDCC-*m*	129.66
15	DCDCC-*n*	129.45
16	CCDCC-*m,n*	129.55

[a] Structural formulas of some representative sequences are shown.

Some resonance splitting from certain ring methine carbons and methylene carbons α to the ring results from ^{13}C–^{19}F coupling through two and three bonds, respectively (e.g., see ^{13}C chemical shifts for compound **3**). The $^2J(^{13}C–^{19}F)$ splitting (10.3 Hz) for >CH– ring carbons is

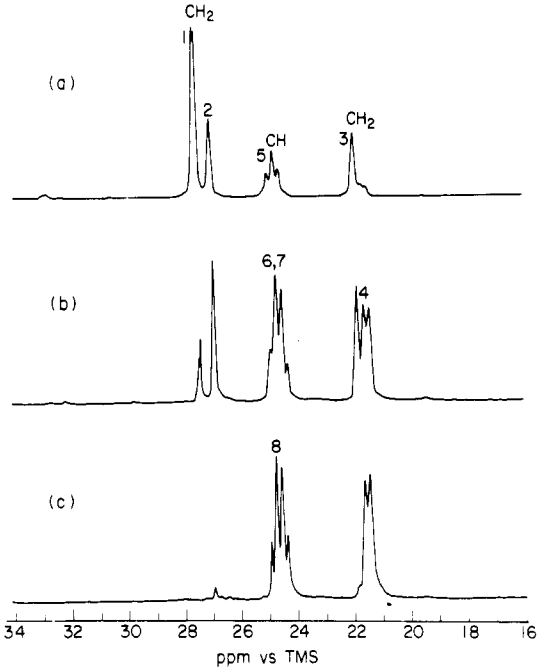

Figure 3. Aliphatic carbon region of 50.3-MHz ^{13}C spectra of *cis*-PBD:CF_2 adducts at (a) 27.6%, (b) 68.4%, and (c) 97.4% double bond conversions, observed in $CDCl_3$ at 50 °C.

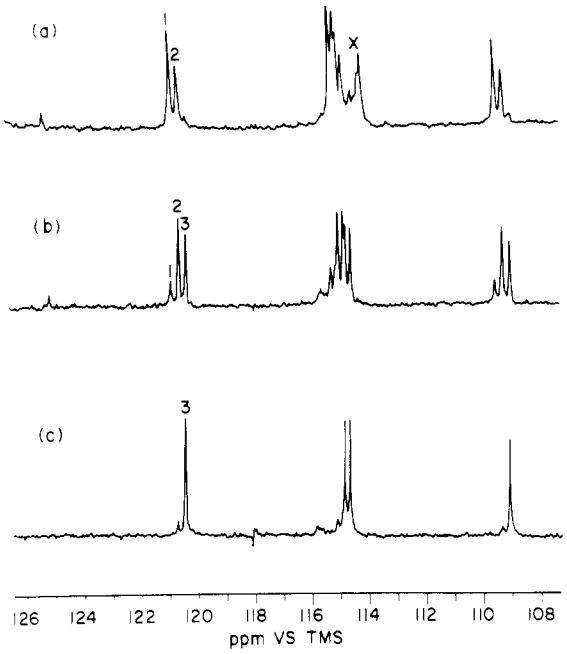

Figure 4. 50.3-MHz ^{13}C spectra of difluoromethylene carbon (>CF_2) of *cis*-PBD:CF_2 adducts at (a) 27.6%, (b) 68.4%, and (c) 97.4% conversions, observed in $CDCl_3$ at 50 °C.

particularly conspicuous at low conversions (ca. 27%) (e.g., spectrum a, Figure 3), since at this conversion no significant monomer sequence effect is likely (most C-centered triads are DCD).

The splitting pattern for the cyclopropyl ring carbon in particular is compounded heteronuclear scalar coupling, stereochemical sequence, and monomer sequence effects (DCD, DCC, and CCC) at intermediate conversions (e.g., spectrum b, Figure 3). At the highest conversion (>97%) virtually all triad monomer sequences are CCC, so that line splittings must now reflect tacticity as well as scalar coupling effects (see spectrum c, Figure 3).

Although the geometrical configuration of the double bond is retained after carbene addition, the stereochemical

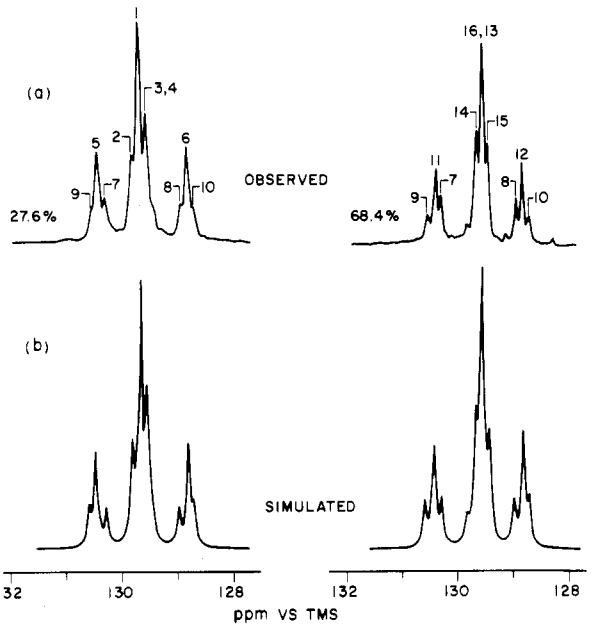

Figure 5. (a) Olefinic carbon region of 50.3-MHz ^{13}C spectra of *cis*-PBD:CF_2 adducts at indicated conversions, observed in $CDCl_3$ at 50 °C. (b) Computer simulation of the ^{13}C olefinic region of the cis adducts for the corresponding conversions. The simulated spectra were generated by using the appropriate chemical shifts and constant linewidths (4 Hz); a Bernoullian statistics was assumed for the simulation.

configuration of the resulting copolymers is random. Adjacent pairs of rings can therefore exist as two nonequivalent stereochemical diads (see below). Of course the enantiomers will be indistinguishable by NMR. Since the C-centered methine carbons are not centrosymmetric (see triad structure CCC, Table III), diad tacticity generates four lines corresponding to the four nonequivalent diastereomers (*rr'*, *mr'*, *rm'*, and *mm'*).

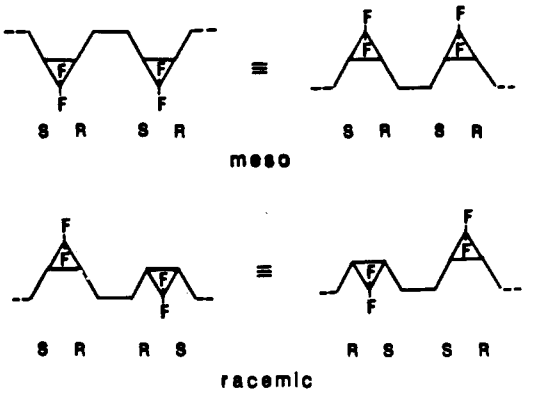

We did not have the capabilities for broad-band fluorine decoupling, so the fine structure pertaining to just sequence isomerism could not be observed. However, the ^{13}C spectral region for the analogous dichlorocarbene adduct of 1,4-*cis*-polybutadiene (*cis*-PBD:CCl_2) at >97% conversion serves as a model. A quartet due to diad tacticity effect was observed for >CH– ring carbons (CCC sequence), supporting our postulations above.[17]

The >CF_2 carbon exhibits triad monomer sequence sensitivity (Figure 4, spectra a, b, and c), which compounds the splittings already present from ^{13}C–^{19}F coupling. The assignments and chemical shifts are shown in Table IV. At intermediate conversions (spectrum b), the three sequences DCD, DCC, and CCC generate 12 lines. Note that each sequence produces four lines from >CF_2 carbons due to an AXY coupling pattern for *cis*-PBD:CF_2 adducts, as

discussed earlier. At >97% conversion, when the triad monomer sequence is mostly CCC, the $>CF_2$ carbon resonance becomes comparable to that from the cis model compound **3** and gives an AXY pattern with $^1J(^{13}C-^{19}F)$ of 283.2 and 282.6 Hz, respectively. It is of interest to note that this carbon remains insensitive to tacticity at all conversions.

By far the most sensitive ^{13}C spectral region involves the olefinic carbon resonances. This region shows sensitivity to pentad monomer sequences, and the expected 16 resonances are dispersed over a narrow frequency domain of ca. 40 Hz. The observed lines with appropriate carbon-type sequences are presented in Table V and Figure 5a.

Several salient features of the olefinic carbon region are apparent. First, the symmetrical appearance of the spectra (Figure 5a) obtains from nearly equal upfield and downfield shifts of the carbon resonances that are directionally nonequivalent, e.g., as in DDDDC or DDDCD (see structures in Table V). Second, the presence of a cyclopropyl ring adjacent to the double bond (as in DDDCD) causes a much larger spread in chemical shift than one that is a next nearest neighbor to the double bond (as in DDDDC). Third, the presence of two cyclopropyl groups as immediate and next nearest neighbors to the double bond (DDDCC) spreads the resonances to even a greater extent (peaks 9 and 10) than one such group placed next to the double bond (DDDCD). Surprisingly, when the double bond is flanked by two cyclopropyl groups the effects appear to cancel, so that the shift perturbation is minimal (see peak 13). Finally at >97% conversion, the residual olefinic carbon resonance from the CCDCC sequence becomes almost indistinguishable from that from *cis*-1,4-PBD.

Similar symmetrical patterns for olefinic carbon splittings have been reported for partially epoxidized 1,4-*trans*-polybutadiene and 1,4-*trans*-polyisoprene.[18,19] The present assignments were aided by analogy with these systems and by observing the change in relative peak intensities with conversion. Computer simulation of the olefinic carbon resonance was done by using the above assignments and constant line width (4 Hz). A good match was obtained when the sequence probabilities were calculated according to random (Bernoullian) statistics. The observed and simulated spectra are compared in Figure 5.

Detailed Carbon-13 Microstructures of *trans*-PBD:CF_2 Adducts. The ^{13}C spectra of *trans*-PBD:CF_2 at 20.7%, 62.6%, and 98.0% conversions are shown in Figures 6–8 and the peak assignments are tabulated in Tables VI–VIII. The carbon splitting patterns in the aliphatic region of *trans*-PBD:CF_2 adducts are very similar to those for *cis*-PBD:CF_2 adducts. These carbon exhibit monomer sequence diads for methylene carbons and triads for the cyclopropyl ring carbons; these also show tacticity influences at the diad level for methine ring carbons in or adjacent to CC sequences. The results are summarized in Table VI and Figure 6.

The $>CF_2$ carbon also shows triad monomer sequences, but no tacticity information. Since the $>CF_2$ carbon is a triplet due to $^1J(^{13}C-^{19}F)$ coupling in *trans*-PBD:CF_2, each triad monomer sequence generates this pattern. In principle the geminal fluorines are no longer equivalent in the unsymmetrical DCC sequence, so an AXY pattern should result in a carbon resonance quartet. In practice, this nonequivalence was not observed. Thus, at intermediate conversions (Figure 7, spectrum b) when all the three C-centered monomer sequences are possible, the $>CF_2$ carbon resonance consists of nine lines.

Table VI
^{13}C Chemical Shifts of Aliphatic Carbons of *trans*-PBD:CF_2 Adducts (See Figure 6)[a]

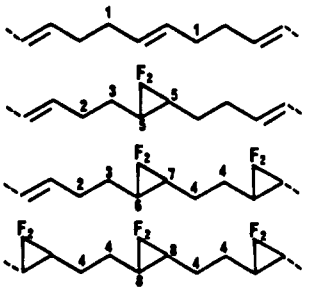

peak assignt	sequence	chem shifts vs. Me_4Si, ppm
1	DD	32.70
2	CD, DC	31.88
3	CD, DC	26.80
4	CC	26.33
	(*m* and *r*)	26.06
5	DCD	28.27
	(mainly triplet)	28.08
		27.89
6	DCC (*m* and *r*)	28.30
7	CCD (*m'* and *r'*)	28.04
		27.89
		27.75
8	CCC	28.13
	(*rr'*, *rm'*, *mm'*, and *mr'*)	27.95
		27.89
		27.72

[a] Structural formulas for sequence assignments are shown.

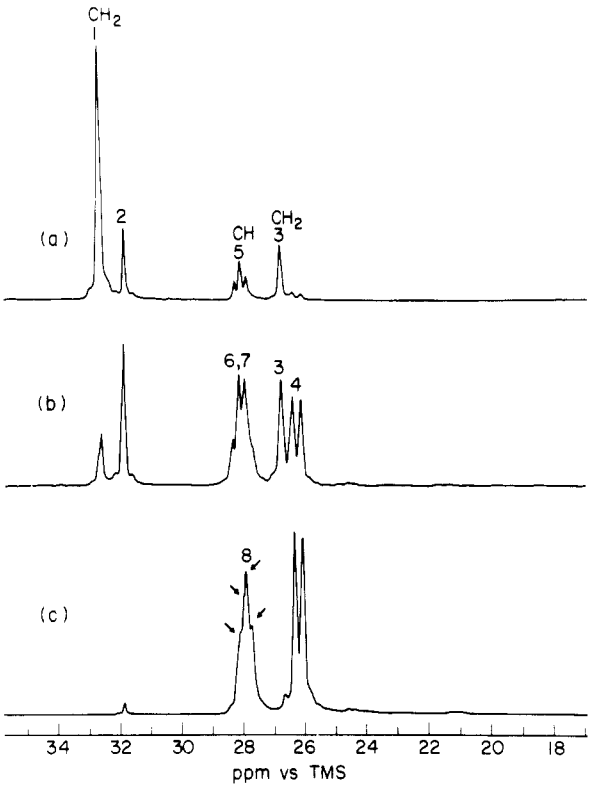

Figure 6. Aliphatic carbon region of 50.3-MHz ^{13}C spectra of *trans*-PBD:CF_2 adducts at (a) 20.7%, (b) 62.6%, and (c) 98.0% double bond conversions, observed in $CDCl_3$ at 50 °C. Arrows in (c) indicate four poorly resolved lines.

The olefinic carbon region shows the splitting pattern expected for pentad monomer sequences. The carbon-type sequences and peak assignments for these carbon reso-

Table VII
^{13}C Chemical Shifts of Difluoromethylene (>CF_2) Carbon of *trans*-PBD:CF_2 (See Figure 7)[a]

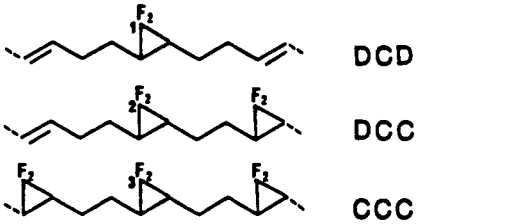

peak design.	assignt	chem shift vs. Me_4Si, ppm
1	DCD	122.33
	(triplets)	116.58
		110.85
2	DCC	121.98
	(triplets)	116.24
		110.51
3	CCC	121.70
	(triplets)	115.97
		110.22

[a] Structural formulas of monomer sequences are shown.

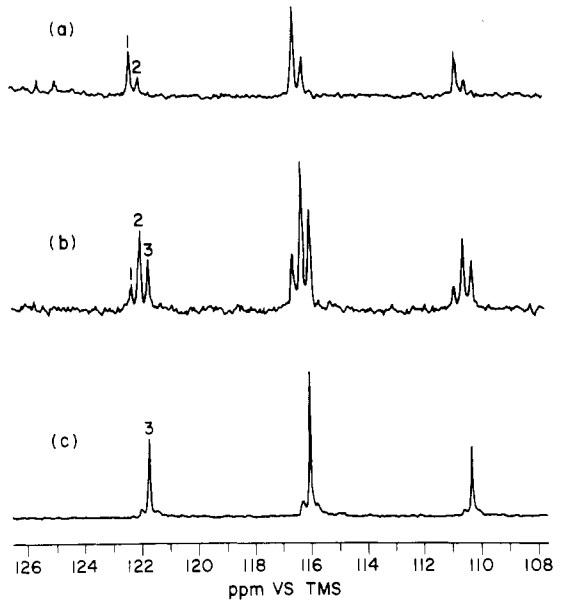

Figure 7. 50.3-MHz ^{13}C spectra of difluoromethylene carbon (>CF_2) of *trans*-PBD:CF_2 adduct at (a) 20.7%, (b) 62.6%, and (c) 98.0% conversions, observed in $CDCl_3$ at 50 °C.

nances in *trans*-PB:CF_2 were deduced like those for the *cis*-PBD:CF_2 case. The results are compiled in Table VIII and shown in Figure 8.

Fluorine-19 Spectra of *cis*- and *trans*-PBD:CF_2 Adducts. Fluorine-19 NMR spectra of model compounds and the polymer adducts were recorded at 188.2 and 470.5 MHz at ambient temperature. The ^{19}F chemical shift assignments for the polymers are based on the resonances for model compounds **3** and **4**.

The nonequivalence of the geminal fluorines in the cis model compound is clearly illustrated by structure **3**, where the corresponding resonances are separated by ca. 30 ppm. The fluorine syn to both backbone methylene carbons has two three-bond interactions γ(C), γ(C) and is strongly shielded with respect to the anti, anti fluorine, which has γ(H), γ(H) interactions. A γ-gauche effect that moves fluorine resonances upfield has been noted in other fluoropolymers.[20] Thus the fluorine spins in cis compound **3** form an AX system and exhibit a doublet of doublets, with $\nu_{syn,syn}$ = −126.0 ppm, $\nu_{anti,anti}$ = −155.7 ppm, and $^2J(^{19}F-^{19}F)$ = 153 Hz. Geminal fluorines having similar nonequivalence owing to different steric environments have been reported in the literature.[21] Compound **4**, *trans*-1,2-di-*n*-butyl-3,3-difluorocyclopropane, has a twofold symmetry axis so the geminal fluorines are equivalent and appear as a singlet at −140.5 ppm (almost in the middle of the

Table VIII
^{13}C Chemical Shifts of Olefinic Carbons of *trans*-PBD:CF_2 (See Figure 8)[a]

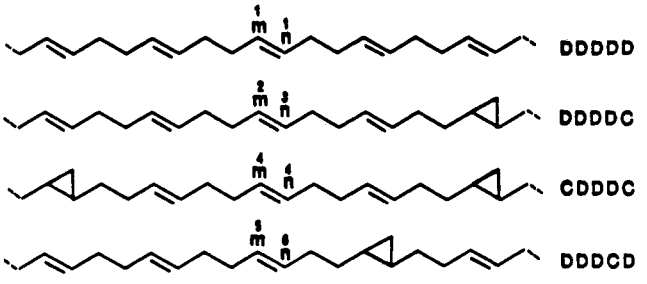

peak assignt	C-type sequence	chem shift vs. Me_4Si, ppm
1	DDDDD-*m,n*	130.06
2	DDDDC-*m*	130.18
3	DDDDC-*n*	129.91
4	CDDDC-*m,n*	129.91
5	DDDCD-*m*	130.94
6	DDDCD-*n*	129.24
7	CDDCD-*m*	130.81
8	CDDCD-*n*	129.35
9	DDDCC-*m*	131.03
10	DDDCC-*n*	129.10
11	CDDCC-*m*	130.93
12	CDDCC-*n*	129.23
13	DCDCD-*m,n*	130.09
14	DCDCC-*m*	130.20
15	DCDCC-*n*	129.96
16	CCDCC-*m,n*	130.11

[a] Structural formulas of some representative sequences are shown.

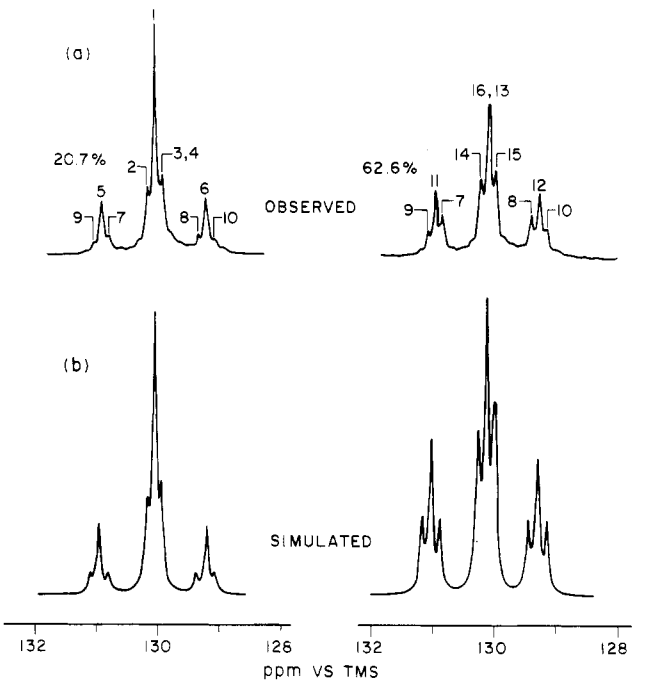

Figure 8. (a) Olefinic carbon region of 50.3-MHz ^{13}C spectra of *trans*-PBD:CF_2 adducts at indicated conversions, observed in $CDCl_3$ at 50 °C. (b) Computer simulation of the ^{13}C olefinic region of the trans adducts for the corresponding conversions. The simulated spectra were generated by using the appropriate chemical shifts and constant linewidths (4 Hz); a Bernoullian statistics was assumed for the simulation.

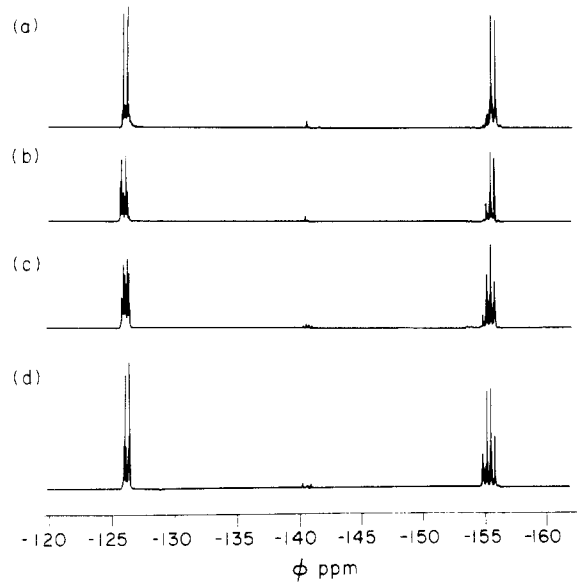

Figure 9. 470.5-MHz ^{19}F NMR spectra of *cis*-PBD:CF_2 adducts at (a) 18.1%, (b) 27.6%, (c) 68.4%, and (d) 97.4% conversions observed in $CDCl_3$ at room temperature.

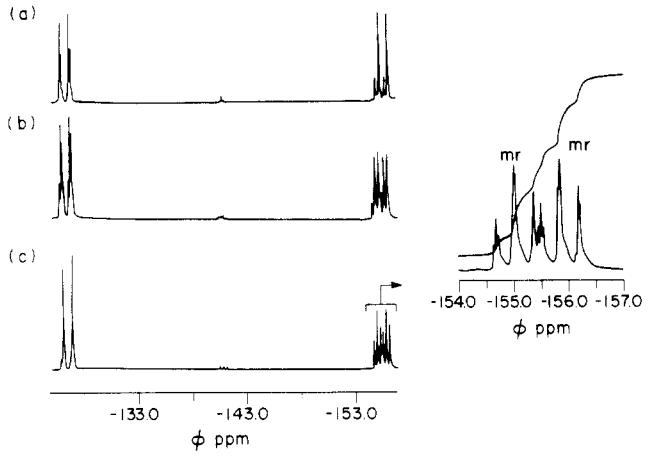

Figure 10. 188.22-MHz ^{19}F NMR spectra of *cis*-PBD:CF_2 adducts at (a) 27.6%, (b) 68.4%, and (c) 97.4% conversions, observed in $CDCl_3$ and at room temperature. The upfield ^{19}F region of *cis*-PBD:CF_2 adduct at >97% conversion (spectrum c) is expanded at the right-hand-most corner which indicates stereochemical triads.

fluorine spectrum for compound **3**). Both fluorines now have the same γ(C), γ(H) interactions (see structure **4**).

Comparison of the fluorine-19 NMR of *cis*- and *trans*-PBD:CF_2 adducts at low conversions (18% and 20%, respectively, where there are minimal sequence effects) reveals a very close resemblence of the spectrum of each isomer with that of the model compound (for example, see Figures 9a and 11a). Thus the fluorine chemical shifts of the adducts can be readily assigned. The cis adduct exhibits an AX spin system (doublets centered at −125.9 and −155.8 ppm, with $^2J(^{19}F-^{19}F)$ = 152.9 Hz), whereas the trans adduct gives the expected singlet at −140.1 ppm. ^{19}F NMR analysis proved to be a very sensitive probe of the geometry of the :CF_2 adducts, owing to the marked difference in spectra from cis and trans isomers. Examination of the ^{19}F spectra of all adducts (e.g., see Figures 9, 10, and 11) verifies the conclusion made earlier from ^{13}C NMR spectra that the addition reaction preserves geometrical isomerism.

Detailed Fluorine-19 Microstructures of *cis*-PBD:CF_2 Adducts. Figures 9 and 10 show the 470.5- and 188.22-MHz ^{19}F spectra of several adducts of *cis*-PBD.

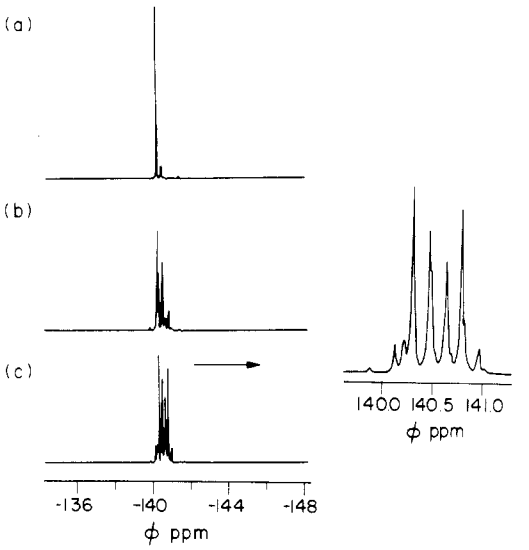

Figure 11. 470.5-MHz ^{19}F NMR spectra of *trans*-PBD:CF_2 adducts at (a) 20.7%, (b) 62.6%, and (c) 98.0% double bond conversions, observed in $CDCl_3$ at room temperature. The upper right-hand corner shows the expansion of spectrum c at >98% conversion.

With increasing conversion sequence effects are manifested by additional fine structure in the spectra. Spectra obtained at 470.5 MHz appear to have less fine structure than those recorded at 188.22 MHz, since scalar coupling is more apparent at the lower field strength.

The additional fine structure resolved at intermediate conversions can be explained by monomer sequence triads. At 27.6% double bond conversion, DCD and DCC sequences are distinguishable (spectrum a, Figure 10), giving rise to two AX quartets. At higher conversions (e.g., 68%), all three C-centered monomer triads have appreciable effects. Finally, at >97% conversion the monomer sequence is mostly CCC and stereochemical information at the triad level becomes obvious, especially in the upfield region of the spectrum (spectrum c, Figure 10). The downfield region suffers from overlapping lines, so that tacticity information is poorly resolved. It is interesting to note the different sensitivities of the geminal fluorines to their stereochemical environment. We postulate that the more shielded fluorine, syn to both backbone methylene carbons (γ(C), γ(C)), is more sensitive since the γ(C) interaction experiences perturbations in backbone conformation more than the γ(H) interactions suffered by the anti, anti fluorine.

Appropriate expansion and careful integration of the upfield region (see Figure 10) reveal at least three sets of principal resonances (spectral width ca. 2 ppm) that are assigned to iso, hetero, and syndio triad stereosequences; the additional fine structures at −155.5 and −154.65 ppm may arise from either stereochemical pentads or long-range $^{19}F-^{19}F$ coupling. The tacticity is Bernoullian with $p(m)$ = 0.5.

Detailed Fluorine-19 Microstructures of *trans*-PBD:CF_2 Adducts. In the case of *trans*-PBD:CF_2 adducts the 470.5-MHz ^{19}F NMR spectra provide more information than those obtained at 188.22 MHz and will be discussed in terms of microstructure. The spectra in Figure 11 indicate monomer sequence and tacticity influences at the triad level. At low conversion when the cyclopropyl groups are fairly isolated from each other, the geminal fluorines are equivalent, giving a singlet. At higher conversions, the fluorines are no longer equivalent owing to sequence effects and form an AB spin system. Spectrum b in Figure 11 is highly complex because of fine structure

from both monomer and stereosequences. However, spectrum c in this Figure shows the simplification achieved at >98% conversion, where nine well resolved lines appear. These lines evolve from stereochemical triads; the heterosteric geminal fluorines in *mr* and *mm* environments give rise to AB quartets, whereas the homosteric geminal fluorines in the symmetrical *rr* environment give a singlet. More detailed ^{19}F assignments of these triad components are not made in the present study.

Conclusions

Difluorocarbene generated from $PhHgCF_3$ under mild, neutral conditions adds to *cis*- and *trans*-1,4-polybutadienes very efficiently with retention of double bond configuration. These adducts can be prepared with any desired level of the geminal difluorocyclopropane moiety, and form a new class of fluorocopolymers. Complete conversion results in the structural equivalent of a 1:1 (ethene-3,3-difluorocyclopropene) copolymer.

The mode of difluorocarbene addition to the polybutadienes is strictly random in both monomer and stereosequence. Thus the crystallinity initially present in *trans*-PBD is destroyed at intermediate conversions, and studies are presently under way to characterize additional properties of these materials.

Acknowledgment. We are grateful to Dr. P. Mirau for help with NMR experiments, to L. Johnson for TGA analyses, to M. Y. Hellman for providing molecular weights, and to J. M. Kometani for assistance in the laboratory.

Registry No. 3, 99966-95-7; 4, 99966-96-8; $PhHgCF_3$, 24925-18-6.

References and Notes

(1) Komoroski, R. A.; Horne, S. E., Jr.; Carman, C. J. *J. Polym. Sci., Polym. Chem. Ed.* **1983**, *21*, 89. See also: Carman, C. J.; Komorski, R. A.; Horne, S. E., Jr. "NMR and Macromolecules"; Randall, J. C., Ed.; American Chemical Society: Washington, DC, 1984; ACS Symp. Ser. No. 247, 1984, Chapter 11, p 167.
(2) Hummel, K.; Martl, M. G.; Chemelli, R.; Greiser, H.; Wukovnig, S.; Zekoll, H. *Makromol. Chem.* **1984**, *185*, 2489 and references therein.
(3) Olsen, D. A.; Osteraas, A. J. *J. Appl. Polym. Sci.* **1969**, *13*, 1523. Osteraas, A. J.; Olsen, D. A. *Nature (London)* **1969**, *221*, 1140.
(4) Rinehart, R. E.; Smith, H. P. "Macromolecular Syntheses"; Wiley: New York, 1978; Collect Vol. 1, p 125.
(5) Seyferth, D.; Mui, J. Y.-Pui; Gordon, M. E.; Burlitch, J. M. *J. Am. Chem. Soc.* **1965**, *87*, 681. Seyferth, D.; Hopper, H. P.; Murphy, G. J. *J. Organometal. Chem.* **1972**, *46*, 201.
(6) Levitt, M. H.; Freeman, R. *J. Magn. Reson.* **1979**, *33*, 473.
(7) Doddrell, D. M.; Pegg, D. T.; Bendall, M. R. *J. Magn. Reson.* **1982**, *48*, 323.
(8) Mitsch, R. A. *J. Am. Chem. Soc.* **1965**, *87*, 758. Burton, D. J.; Naae, D. G. *Ibid.* **1973**, *95*, 8467. For a comprehensive review on the various sources of difluorocarbene, see: Burton, D. J.; Hahnfeld, J. L. "Fluorine Chemistry Reviews"; Tarrant, P., Ed.; Marcel Dekker: New York, 1977; Vol. 8, Chapter 4, p 153.
(9) Kirmse, W. "Carbene Chemistry", 2nd ed.; Academic Press: New York, 1971; Chapter 4, p 129.
(10) Dias, A. J.; McCarthy, T. J. *Polym. Prepr. (Am. Chem. Soc., Div. Polym. Chem)* **1985**, *26*, 161.
(11) Skell, P. S.; Woodworth, R. C. *J. Am. Chem. Soc.* **1956**, *78*, 4496.
(12) Fox, T. G.; Loshaek, S. *J. Polym. Sci.* **1955**, *15*, 371.
(13) Schaefer, J. "Topics in Carbon-13 NMR Spectroscopy"; Levy, G. C., Ed.; Wiley: New York, 1974; Vol. 1, Chapter 4, p 150.
(14) Schaefer, J. "Structural Studies of Macromolecules by Spectroscopic Methods"; Ivin, K. J., Ed.; Wiley: New York, 1976; Chapter 11, p 208.
(15) Grant, D. M.; Paul, E. G. *J. Am. Chem. Soc.* **1964**, *86*, 2984.
(16) Lindeman, L. P.; Adams, J. Q. *Anal. Chem.* **1971**, *43*, 1245.
(17) Siddiqui, S.; Cais, R. E. to be published.
(18) Schilling, F. C.; Bovey, F. A.; Tseng, S.; Woodward, A. E. *Macromolecules* **1983**, *16*, 808.
(19) Schilling, F. C.; Bovey, F. A.; Anandakumaran, K.; Woodward, A. E. *Macromolecules* **1985**, *18*, 2688.
(20) Tonelli, A. E.; Schilling, F. C.; Cais, R. E. *Macromolecules* **1982**, *15*, 849.
(21) Jefford, C. W.; Kebengale, T.; Kovacs, J.; Burger, U. *Helv. Chim. Acta* **1974**, *57*, 104. See also ref 22 for a similar chemical shift spread due to nonequivalent fluorines.
(22) Ando, T.; Yamanaka, H.; Funasaka, W. *Tetrahedron Lett.* **1967**, 2587.

Formation and Relaxation of an Excited Complex in a Polymer

S. Tazuke,* Y. Higuchi, No. Tamai, N. Kitamura, Na. Tamai,† and I. Yamazaki†

Research Laboratory of Resources Utilization, Tokyo Institute of Technology, 4259 Nagatsuta, Midori-ku, Yokohama 227, Japan. *Received June 5, 1985*

ABSTRACT: The dynamic fluorescence spectroscopy of an excimer-forming polymer (I) and an exciplex-forming polymer (II) is reported in comparison with the corresponding dimer model (III) and monomer model (IV), respectively, in dilute solution. The rise profile of intrapolymer excimer in I is faster than that of III, although diffusion of polymer-bonded chromophores is slower than for the small molecule. The reason is believed to be the high local concentration of chromophores in I. In the case of exciplex formation by II, the mode of excited-state interaction is mostly interpolymer and the formation of the exciplex is completed within a time of the order of 100 ps. The corresponding monomer model (IV) forms the exciplex more slowly. Loose polymer association prior to excitation accounts for the fast rise of the exciplex emission in II. The time-resolved fluorescence of II shows a gradual red shift of the exciplex emission beyond 100 ns, whereas IV does not exhibit this shift. This is an indication that solvation and other relaxation processes forming the stable exciplex state in II are slow. Also, excimer formation by I does not show a time-dependent wavelength shift since the relaxation of the excimer is less than that of the exciplex. Fluorescence lifetime measurements with a fixed wavelength for the polymer must therefore be made with care.

Excited-state interaction in polymer systems is a rapidly growing area of research as a basis for photopolymers and for understanding photophysicochemical phenomena in molecular aggregate systems.[1] Energy migration and transfer, interaction of the excited chromophore with molecules in the ground state leading to excimer formation, exciplex formation, dimerization, electron transfer, and other phenomena are unit processes of photoresponsive functions in polymers and molecular aggregate systems. These excited-state interactions are useful probes not only for photopolymers but also for the study of polymer

† Institute for Molecular Science, Myodaiji, Okazaki 444, Japan.

0024-9297/86/2219-0603$01.50/0